

Boundary and Context Aware Training for CIF-based Non-Autoregressive End-to-end ASR

Fan Yu¹, Haoneng Luo¹, Pengcheng Guo¹, Yuhao Liang¹, Zhuoyuan Yao¹, Lei Xie¹, Yingying Gao²,
Leijing Hou², Shilei Zhang²

¹Audio, Speech and Language Processing Group (ASLP@NPU), School of Computer Science,
Northwestern Polytechnical University, Xi'an, China

²China Mobile Research Institute

fyu@npu-aslp.org, lxie@nwpu.edu.cn

Abstract

Continuous integrate-and-fire (CIF) based models, which use a soft and monotonic alignment mechanism, have been well applied in non-autoregressive (NAR) speech recognition and achieved competitive performance compared with other NAR methods. However, such an alignment learning strategy may also result in inaccurate acoustic boundary estimation and deceleration in convergence speed. To eliminate these drawbacks and improve performance further, we incorporate an additional connectionist temporal classification (CTC) based alignment loss and a contextual decoder into the CIF-based NAR model. Specifically, we use the CTC spike information to guide the learning of acoustic boundary and adopt a new contextual decoder to capture the linguistic dependencies within a sentence in the conventional CIF model. Besides, a recently proposed Conformer architecture is also employed to model both local and global acoustic dependencies. Experiments on the open-source Mandarin corpora AISHELL-1 show that the proposed method achieves a comparable character error rate (CER) of 4.9% with only 1/24 latency compared with a state-of-the-art autoregressive (AR) Conformer model.

Index Terms: Non-autoregressive, end-to-end speech recognition, continuous integrate-and-fire

1. Introduction

End-to-end (E2E) models have achieved great success in automatic speech recognition (ASR) due to their effectiveness in sequence-to-sequence modeling [1–5]. Compared with the traditional hybrid systems [6, 7], E2E models can not only simplify the model training process and reduce the computational cost but also achieve competitive or even better recognition accuracy. However, most state-of-the-art E2E models follow an autoregressive (AR) fashion and recursively generate the next token based on the previously generated tokens. Thus, it will take at least L iterations to generate an L -length output sequence, resulting in a complex computation and a large latency with the increment of sequence length. In contrast, the non-autoregressive (NAR) models make a conditional independence assumption among the output tokens and no longer rely on the time relationship from left to right, which can generate L tokens in parallel with a constant $K (<< L)$ iterations.

Non-autoregressive models are originally proposed in neural machine translation (NMT) tasks and have been applied ASR very recently. The major difficulties of non-autoregressive model consist of the following two aspects: the accurate prediction of target sequence length and the parallel inference of decoder. Introducing a length prediction network behind the

encoder [8–10] or estimating an empirical target length according to the source sequence [11] are two typical length prediction approaches. However, both methods will bring redundant computations and cannot guarantee the accuracy of the predicted lengths for varied-length datasets that are common in real applications. Since connectionist temporal classification is good at learning frame-wise latent alignments between the input speech and output tokens, more and more studies get rid of the cumbersome length estimation and focus on incorporating the CTC into non-autoregressive models. In [12], Tian *et al.* proposed a spike-triggered based non-autoregressive method, which uses the encoded states corresponding to the CTC spikes as the input of decoder. Although the decoder can easily perform parallel computation with these methods, the length mismatch between the CTC spikes and target sequence will lead to a computation problem of cross-entropy (CE) loss. Inspired by the masked language modeling, Mask-CTC [13] initialized the input target sequence with masked ground-truth during the training and masked token-level CTC outputs during the inference, respectively. The idea of the model is to infer the masked tokens by the decoder and iteratively refine them. In addition to Mask-CTC, Imputer [14] effectively models context dependencies and CASS-NAT [15] generates token-level acoustic embedding through CTC alignment sequence, which are also confronting a redundant computation problem caused by a longer sequence.

Recently, a novel non-autoregressive framework named continuous integrate-and-fire (CIF) [16] was proposed, which includes a soft and monotonic alignment mechanism and extracts the acoustic embedding corresponding to each label. It can not only determine the length of the prediction sequence but also effectively integrate the information within the acoustic boundary of each label. Although CIF is more accurate in computing the length of the entire sequence, there is a deviation in the prediction of the local acoustic boundary of each label. In this paper, in order to improve the accuracy of CIF prediction of the label acoustic boundary (e.g. character boundary in Chinese), we propose a new auxiliary function to constrain the acoustic boundary of each label by using the spike information and alignment states of CTC. Besides, we also use the recently proposed Conformer encoder to enhance the representation of the acoustic information, which has better local and global modeling capabilities than Transformer. Finally, we introduce a new contextual decoder to improve the linguistic and contextual dependencies within the target sequences. Evaluated on the open-source Mandarin corpora AISHELL-1, our proposed method achieves a comparable character error rate (CER) of 4.9% with only 1/24 latency compared with a state-of-the-art autoregres-

sive Conformer model.

The rest of this paper is organized as follows. Section 2 introduces non-autoregressive continuous integrate-and-fire (CIF) model. Section 3 describes our proposed method. Section 4 presents our experimental setup and results. The conclusions and future work will be given in Section 5.

2. Non-autoregressive Continuous Integrate-and-Fire (CIF)

A conventional autoregressive framework receives a feature sequence $\mathbf{x} = [x_1, \dots, x_t, \dots]$ and produces output tokens $\mathbf{y} = [y_1, \dots, y_i, \dots]$ one-by-one, as follows:

$$P_{\text{ar}}(\mathbf{y}|\mathbf{x}) = \prod_{l=1}^L P_{\text{att}}(y_l|y_{<l}, \mathbf{x}). \quad (1)$$

With the previously generated tokens $y_{<l}$, it estimates the output token y_l at each time step condition, resulting in a low parallelization and slow inference speed. By contrast, a non-autoregressive model can produce output tokens in parallel. During the inference, it will generate the probability distribution of \mathbf{y} independently according to the input feature, without strict time dependence requirement. Mathematically, a non-autoregressive model can be defined as:

$$P_{\text{nar}}(\mathbf{y}|\mathbf{x}) = \prod_{l=1}^L P_{\text{att}}(y_l|\mathbf{x}). \quad (2)$$

As shown in Fig. 1, the left part shows the structure of CIF module. The CIF module is a middleware employed in the encoder-decoder framework, and its output, replacing the label embedding, is directly used as the input of the decoder to achieve parallel non-autoregressive decoding. At each encoder step, CIF receives the current state and its information weight α of the encoder to compute an acoustic embedding of each label. Weight α scales the amount of acoustic information in \mathbf{h} at each time step, and it is accumulated forward from left to right until the accumulated weight reaches the threshold β , which means an acoustic boundary of a label is determined. Thus, CIF is able to provide a soft alignment between acoustic frames and target labels. The weight of acoustic boundary position contains two parts of acoustic information: one for the integration of current label on relevant encoder steps, and the other is used for the accumulation of acoustic information of the next label, which is used to obtain the acoustic embedding \mathbf{c} of the corresponding label by weighted summation with the relevant encoded output \mathbf{h} .

In order to improve the accuracy of sequence length prediction by CIF module, Dong *et al.* proposed a quantity loss to supervise the CIF-based model to predict the quantity of integrated embedding closer to the quantity of targeted label sequence [16]. Quantity loss \mathcal{L}_{qua} is defined as Eq. (3), where \tilde{S} is the length of the targets \mathbf{y} .

$$\mathcal{L}_{\text{qua}} = \left| \sum_{u=1}^U \alpha_u - \tilde{S} \right|. \quad (3)$$

3. Proposed Method

Our proposed approach is based the CIF module with substantial improvements to obtain more accurate acoustic boundary and to better capture context information. Specifically, we adopt a CTC module to guide the learning of acoustic boundary and plug a novel context decoder to the CIF decoder to better capture the token relationship, as shown in Fig. 1. We use Conformer as encoder as it has better local and global modeling

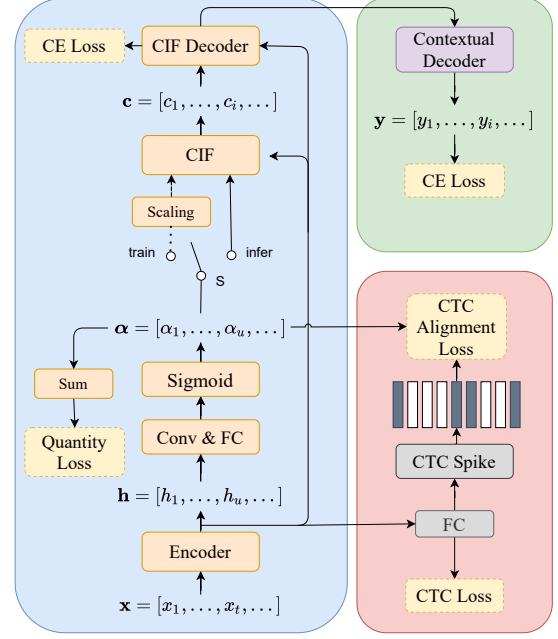


Figure 1: The architecture of our CIF-based non-autoregressive model is used for the ASR task. The left part shows the structure of CIF module, and the right part shows the contextual decoder and CTC alignment loss.

capabilities than oracle Transformer. Moreover, unlike the original CIF which only uses acoustic embedding of CIF module as in Eq. (4), we fire both the acoustic embedding \mathbf{c} and encoder output \mathbf{h} to the decoder to predict the probability of output tokens $\mathbf{y} = [y_1, \dots, y_i, \dots]$ in parallel as in Eq. (5). We notice that this can lead to a small gain in recognition performance.

$$P(\mathbf{y}|\mathbf{c}) = \text{Decoder}(\mathbf{c}), \quad (4)$$

$$P(\mathbf{y}|\mathbf{c}, \mathbf{h}) = \text{Decoder}(\mathbf{c}, \mathbf{h}). \quad (5)$$

3.1. Conformer Encoder

Our encoder block follows the Conformer [17] architecture, which combines both convolution neural networks (CNNs) and multi-head self attention (MHSA) modules to model both local and global dependencies of an audio sequence in a parameter-efficient way. By adopting Conformer, we expect to improve the prediction performance of CTC and CIF modules as well. Besides, including the relatively positional encoding to MHSA modules also allows the self-attention layer to generalize better on variable lengths of input sequences.

3.2. CTC alignment loss

Due to the speaker's speaking rate, accent, silence and noise, which often happen in real applications, the alignment learning strategy of CIF may results in inaccurate acoustic boundary estimation, which severely influence the convergence speed. To figure out these problems and improve the performance, we present an additional CTC alignment loss function (as shown in Fig 1) to guide the CIF-based model to predict the acoustic boundary closer to the actual boundary by making full use of the CTC spike information. Since the CTC spike is usually within the acoustic boundary of the label, we can roughly determine the boundary of a label by two consecutive CTC spikes. The CTC spike module is shown in Fig. 2. Given a CTC spike sequence $P_s = [0, 0, 1, 0, 0, 1, 0, 1, 0, \dots]$, where 1 means the

probability of non-blank token is greater than a specific threshold θ , we constrain the CIF weight α according to the label boundary sequence $P_b = [-1, 2, 5, 7, \dots]$, which is generated from the spike sequence P_s . The additional alignment loss \mathcal{L}_{ali} can be formulated as:

$$L_{\text{ali}} = \sum_{i=0}^L \left| \sum_{j=P_b(i)+1}^{P_b(i+1)} \alpha(j) - 1 \right|. \quad (6)$$

where L is the length of the targets \mathbf{y} . By providing the alignment label boundary constraints, we combine the boundary information predicted by CTC and CIF to promote the model to learn the label boundary position in a parameter-efficient way.

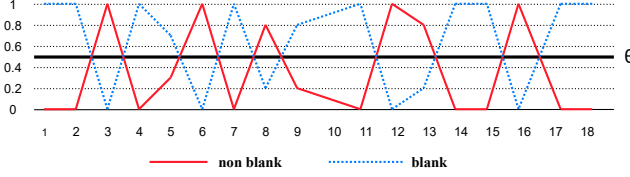


Figure 2: The spike-like trigger probability curve. The red curve represents the non-blank label probability, and the solid black line represents the trigger threshold θ . The probability of a non-blank token greater than θ is a spike.

3.3. Contextual decoder

To further help the CIF decoder to capture the token relationship, we propose a contextual decoder after CIF decoder to capture the contextual relationship within a sequence. Although the outputs of the CIF decoder can be seen as an integrated representation of acoustic and linguistic information corresponding to the tokens, the context correlation between tokens is weak. The contextual decoder leverages a stack of self-attention blocks, and its input of the query, key, and value is the output of CIF decoder, which does not require the acoustic output representation of encoder since it already contains enough acoustic information of each token. Moreover, considering the deep layers of the model, we calculate the cross-entropy (CE) loss of between the outputs of CIF decoder and contextual-decoder to assist the backward update of the gradient and speed up the convergence. The cross-entropy loss can be formulated as $\mathcal{L}_{\text{CE}} = \mathcal{L}_{\text{CE}}(\mathbf{y}') + \mathcal{L}_{\text{CE}}(\mathbf{y}'')$, where \mathbf{y}' and \mathbf{y}'' indicate CIF decoder output and contextual decoder output respectively. Note that our model with contextual decoder needs to train more epochs or use a pre-trained encoder to speed up the model convergence.

3.4. Training strategy

As described in section 2, considering the accuracy of sequence length prediction for CIF module and the lack of left-to-right constraints for the attention model, our model also adopts the quantity loss and CTC loss. In addition, we introduce a CTC alignment loss \mathcal{L}_{ali} to further promote the learning of acoustic boundary as described in Section 3.2. Finally, we also compute the CE loss \mathcal{L}_{CE} for the CIF decoder and the contextual decoder to boost the model learning. Therefore, our model is trained with a combination of four different losses:

$$\mathcal{L} = \mathcal{L}_{\text{CE}} + \lambda_1 \mathcal{L}_{\text{ali}} + \lambda_2 \mathcal{L}_{\text{CTC}} + \lambda_3 \mathcal{L}_{\text{qua}}, \quad (7)$$

where λ_1 , λ_2 and λ_3 are interpolation factors. In this study, these hyper-parameters are set to 1 and the effect of these auxiliary functions will also be investigated in the following experiments.

4. Experiments

4.1. Dataset

In this work, we carried out all experiments on a publicly available Mandarin speech corpus AISHELL-1 [18], which consists of 150 hours of speech recorded by 340 speakers for training, 18 hours of speech recorded by 40 speakers for development and about 10 hours speech for test. The speakers of the three data sets were not overlapped and recorded in a relatively quiet indoor environment.

4.2. Experimental Setup

In our work, we use 80-dimensional log Mel-filter bank features (FBank) computed on 25ms window with 10ms shift and 3-dimensional pitch features [19] as the input. We use 4231 characters extracted from the training transcript as the modeling units.

We use the ESPnet [20, 21] toolkit to build our CIF-based non-autoregressive model, which contains 12 encoder layers, 6 CIF decoder and 6 contextual decoder layers. The dimension of attention and feed-forward layer is 256 with 4 heads and 2048, respectively. We use the Adam optimizer [22] to train the model for 80 epochs. The warm-up [23] is used for the first 25,000 iterations. SpecAugment [24] and speed perturbation [25] with the factor of 0.9 and 1.1 are also applied to avoid over-fitting.

For a more fair comparison, we re-implemented the CTC and Spike-Triggered [12] models with the same parameters and structure as ours model. Besides, we also use the Conformer [17] encoder to systems. To compare the inference speed of each model, we compute real-time factor (RTF) on the test set. All the experiments are conducted on a single NVIDIA RTX 2080Ti GPU.

4.3. Results

From Table 1. we can find the proposed Conformer-CIF-based model outperforms chain model (7.6%) [18] on test set and even reaches the state-of-the-art autoregressive Conformer model. In terms of character error rates (CERs), Conformer-CIF-based model is consistent on the dev set and increases only 0.2% on the test set compared with Conformer model. At the same time, our model is, at most, 17 times faster than Conformer model of the decoding speed measured in RTF.

By comparing the results of non-autoregressive models, our Conformer-CIF-based model is superior to other non-autoregressive models in performance with relatively low RTF, which achieves 4.5% and 4.9% of CER on dev set and test set respectively and 0.0166 of RTF on test set. Since the decoding of our model only iterates once to get the result, RTF of our model is very close to that of Conformer-CTC and Conformer-Spike-Triggered model. However, the CIF module determines the boundary to obtain the acoustic embedding representation of each label, so the RTF of our model is slightly larger than that of models.

In addition, we can see that the two new optimization methods significantly improve the performance and convergence speed of our Conformer-CIF-based model with negligible RTF increase. Adopting a new contextual decoder to capture the linguistic dependencies within a sentence, the CER of dev and test set relative decreased by 4.12% and 5.67% respectively. And the additional CTC based alignment loss absolute decreases the CER 0.1% on both dev set and test set, also greatly accelerate the convergence of the model with no RTF increased. In order to fairly compare our full model, we also added contextual

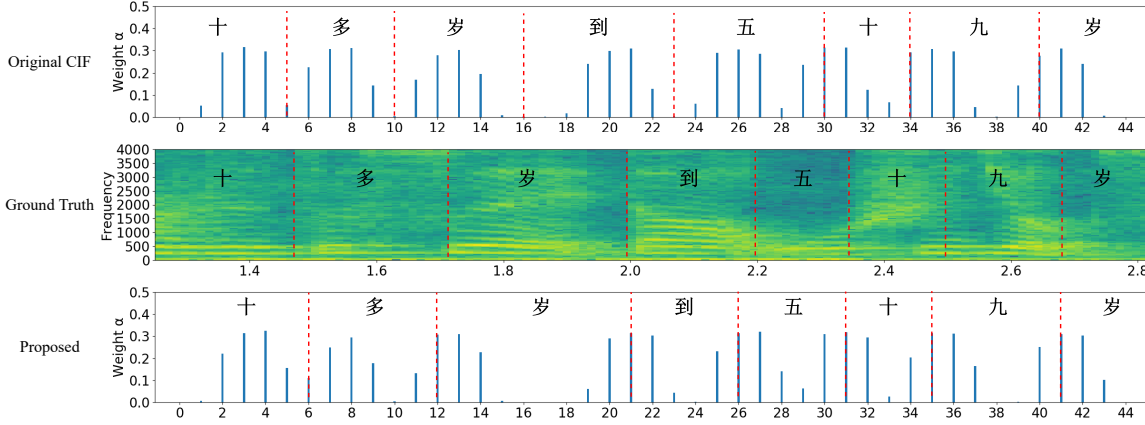


Figure 3: Visualization on the prediction of weight α for each encoded state for the original CIF model (upper) and our CIF model (lower) with contextual decoder and CTC alignment loss. These figures are drawn for the utterance index BAC009S0764W0356 in the AISHELL-1 test set. We find that the original CIF model (upper), as mentioned in [16], is more prone to be located ahead of time, but our CIF model (lower) predicts the boundary of each token more accurately. Red dotted vertical line: character boundary.

decoder to Conformer model. We can see that our proposed non-autoregressive model is nearly 24 times faster than autoregressive Conformer model in RTF with no loss of ASR performance.

Table 1: The character error rates (CERs) of the systems on AISHELL-1. Real-time factor (RTF) is computed as the ratio of the total inference time to the total duration of the test set.

Model	CER (%)		RTF
	Dev	Test	
<i>Autoregressive</i>			
Conformer	4.8	5.1	0.2768
+ Contextual decoder	4.4	4.8	0.4306
Kaldi chain [18]	-	7.6	-
<i>Non-autoregressive</i>			
Transformer-A-FMLM [26]	6.2	6.7	-
Transformer-Insertion [27]	6.1	6.7	-
Transformer-LASO [11]	5.8	6.4	-
Transformer-CASS-NAT [15]	5.3	5.8	-
Conformer-CTC	5.1	5.7	0.0125
Conformer-Spike-Triggered [*] [12]	5.0	5.6	0.0152
<i>Non-autoregressive (proposed)</i>			
Conformer-CIF-based	4.8	5.3	0.0166
+ Contextual decoder	4.6	5	0.0181
+ CTC alignment loss	4.5	4.9	0.0182

*: This models is re-implemented by ourselves with the same parameter structure as our model.

As can be seen from Fig 3, the upper and lower parts show the weight α for each encoded state, and the sum of the weight α within each boundary is equal to threshold β . The upper part is the original CIF model, while the lower part is the CIF model with contextual decoder and CTC alignment loss module. Between these parts is the marked spectrogram of the audio sequence. Besides, we find that the original CIF model, as mentioned in [16], is more prone to be located ahead of time, but our CIF model predicts the boundary of each label extremely accurately. CTC alignment loss plays a significant role to use the CTC spike information to guide the learning of acoustic boundary in the conventional CIF model, which can not only accelerate the convergence speed of the model but also enhance the prediction accuracy of the label boundary range and the whole sequence length that further reduce the insertion and deletion

errors.

After analyzing the decoding results, we note that most of the errors of prediction sequences are similar pronunciation substitution errors as shown in Fig 4. The upper part shows the ground truth sequence, and the middle part shows CIF-based inference sequence. Considering the lack of context-dependency within a sentence, we adopt the contextual-decoder to improve the linguistic and contextual relationship to recover the similar pronunciation substitution errors. As shown in the lower part of Fig 4, the substitution error was successfully corrected.

Ground truth

重点突破棉花油菜甘蔗收获机械化瓶颈

CIF-based inference

重点突破棉花油菜干着收获机械化瓶颈

CIF-based with contextual decoder

重点突破棉花油菜甘蔗收获机械化瓶颈

Figure 4: Decoding example for BAC009S0903W0239 in Aishell1 test set. Red indicates characters with errors and blue indicates ones recovered with a contextual decoder.

5. Conclusions

In this paper, we proposed a new non-autoregressive end-to-end speech recognition framework based on CIF. The core idea of the framework is to determine the acoustic boundary of each label and then get the acoustic embedding of the corresponding label as decoder input so as to achieve parallel and efficient decoding. Meanwhile, to improve the model performance, we proposed an additional connectionist temporal classification based alignment loss and a contextual decoder into the CIF-based non-autoregressive model. We conducted a series of experiments on public AISHELL-1 corpus, and results demonstrated the efficacy of our approach. As compared with the autoregressive model, CIF based non-autoregressive model achieved low inference latency and comparable performance on AISHELL-1 task. In the future, we will explore the performance of our model on English data sets whose acoustic boundary is more blurred and integrate the external language model into our proposed model.

6. References

- [1] J. Chorowski, D. Bahdanau, D. Serdyuk, K. Cho, and Y. Bengio, "Attention-based models for speech recognition," *arXiv preprint arXiv:1506.07503*, 2015.
- [2] C.-C. Chiu, T. N. Sainath, Y. Wu, R. Prabhavalkar, P. Nguyen, Z. Chen, A. Kannan, R. J. Weiss, K. Rao, E. Gonina *et al.*, "State-of-the-art speech recognition with sequence-to-sequence models," in *Proc. ICASSP*. IEEE, 2018, pp. 4774–4778.
- [3] L. Dong, S. Xu, and B. Xu, "Speech-transformer: a no-recurrence sequence-to-sequence model for speech recognition," in *Proc. ICASSP*. IEEE, 2018, pp. 5884–5888.
- [4] S. Kim, T. Hori, and S. Watanabe, "Joint ctc-attention based end-to-end speech recognition using multi-task learning," in *Proc. ICASSP*. IEEE, 2017, pp. 4835–4839.
- [5] W. Chan, N. Jaitly, Q. Le, and O. Vinyals, "Listen, attend and spell: A neural network for large vocabulary conversational speech recognition," in *Proc. ICASSP*. IEEE, 2016, pp. 4960–4964.
- [6] K. Vesely, A. Ghoshal, L. Burget, and D. Povey, "Sequence-discriminative training of deep neural networks," in *Proc. INTERSPEECH*, 2013, pp. 2345–2349.
- [7] V. Peddinti, D. Povey, and S. Khudanpur, "A time delay neural network architecture for efficient modeling of long temporal contexts," in *Proc. INTERSPEECH*, 2015, pp. 3214–3218.
- [8] J. Lee, E. Mansimov, and K. Cho, "Deterministic non-autoregressive neural sequence modeling by iterative refinement," in *Proc. EMNLP*, 2018, pp. 1173–1182.
- [9] J. Gu, J. Bradbury, C. Xiong, V. O. Li, and R. Socher, "Non-autoregressive neural machine translation," in *Proc. ICLR*, 2018.
- [10] X. Ma, C. Zhou, X. Li, G. Neubig, and E. Hovy, "Flowseq: Non-autoregressive conditional sequence generation with generative flow," in *Proc. EMNLP-IJCNLP*, 2019, pp. 4273–4283.
- [11] Y. Bai, J. Yi, J. Tao, Z. Tian, Z. Wen, and S. Zhang, "Listen attentively, and spell once: Whole sentence generation via a non-autoregressive architecture for low-latency speech recognition," in *Proc. INTERSPEECH*, 2020, pp. 3381–3385.
- [12] Z. Tian, J. Yi, J. Tao, Y. Bai, S. Zhang, and Z. Wen, "Spike-triggered non-autoregressive transformer for end-to-end speech recognition," in *Proc. INTERSPEECH*, 2020, pp. 5026–5030.
- [13] Y. Higuchi, S. Watanabe, N. Chen, T. Ogawa, and T. Kobayashi, "Mask ctc: Non-autoregressive end-to-end asr with ctc and mask predict," in *Proc. INTERSPEECH*, 2020, pp. 3655–3659.
- [14] W. Chan, C. Saharia, G. Hinton, M. Norouzi, and N. Jaitly, "Imputer: Sequence modelling via imputation and dynamic programming," in *Proc. ICML*. PMLR, 2020, pp. 1403–1413.
- [15] R. Fan, W. Chu, P. Chang, and J. Xiao, "CASS-NAT: Ctc alignment-based single step non-autoregressive transformer for speech recognition," in *Proc. ICASSP*, 2021.
- [16] L. Dong and B. Xu, "CIF: Continuous integrate-and-fire for end-to-end speech recognition," in *Proc. ICASSP*. IEEE, 2020, pp. 6079–6083.
- [17] A. Gulati, J. Qin, C.-C. Chiu, N. Parmar, Y. Zhang, J. Yu, W. Han, S. Wang, Z. Zhang, Y. Wu *et al.*, "Conformer: Convolution-augmented transformer for speech recognition," in *Proc. INTERSPEECH*, 2020, pp. 5036–5040.
- [18] H. Bu, J. Du, X. Na, B. Wu, and H. Zheng, "Aishell-1: An open-source mandarin speech corpus and a speech recognition baseline," in *Proc. O-COCOSDA*. IEEE, 2017, pp. 1–5.
- [19] P. Ghahremani, B. BabaAli, D. Povey, K. Riedhammer, J. Trmal, and S. Khudanpur, "A pitch extraction algorithm tuned for automatic speech recognition," in *Proc. ICASSP*. IEEE, 2014, pp. 2494–2498.
- [20] S. Watanabe, T. Hori, S. Karita, T. Hayashi, J. Nishitoba, Y. Unno, N.-E. Y. Soplin, J. Heymann, M. Wiesner, N. Chen *et al.*, "ES-Pnet: End-to-end speech processing toolkit," in *Proc. INTERSPEECH*, 2018, pp. 2207–2211.
- [21] P. Guo, F. Boyer, X. Chang, T. Hayashi, Y. Higuchi, H. Inaguma, N. Kamo, C. Li, D. Garcia-Romero, J. Shi *et al.*, "Recent developments on espnet toolkit boosted by conformer," in *Proc. ICASSP*, 2021.
- [22] D. P. Kingma and J. Ba, "Adam: A method for stochastic optimization," in *Proc. ICLR*, 2015.
- [23] A. Vaswani, N. Shazeer, N. Parmar, J. Uszkoreit, L. Jones, A. N. Gomez, L. Kaiser, and I. Polosukhin, "Attention is all you need," in *Proc. NeurIPS*, 2017, pp. 5998–6008.
- [24] D. S. Park, W. Chan, Y. Zhang, C.-C. Chiu, B. Zoph, E. D. Cubuk, and Q. V. Le, "SpecAugment: A simple data augmentation method for automatic speech recognition," in *Proc. INTERSPEECH*, 2019, pp. 2613–2617.
- [25] T. Ko, V. Peddinti, D. Povey, and S. Khudanpur, "Audio augmentation for speech recognition," in *Proc. INTERSPEECH*, 2015, pp. 3586–3589.
- [26] N. Chen, S. Watanabe, J. Villalba, and N. Dehak, "Listen and fill in the missing letters: Non-autoregressive transformer for speech recognition," *arXiv preprint arXiv:1911.04908*, 2019.
- [27] Y. Fujita, S. Watanabe, M. Omachi, and X. Chan, "Insertion-based modeling for end-to-end automatic speech recognition," in *Proc. INTERSPEECH*, 2020, pp. 3660–3664.